Biochimica et Biophysica Acta, 1067 (1991) 17–28

ADONIS 000527369100290P

BBAMEM 75307

The influence of acyl chain-length asymmetry on the phase transition parameters of phosphatidylcholine dispersions

Hai-nan Lin, Zhao-qing Wang and Ching-hsien Huang

Department of Biochemistry, Health Sciences Center, University of Virginia, Charlottesville, VA (U.S.A.)

(Received 21 March 1991)

Key words: Mixed interdigitated bilayer; Mixed-chain phosphatidylcholine; Phosphatidylcholine; Phase transition; DSC

The influence of acyl chain-length asymmetry on the thermodynamic parameters (T_m, ΔH, and ΔS) associated with the reversible main phase transition of aqueous dispersions prepared from saturated diacyl phosphatidylcholines was studied by high-resolution differential scanning calorimetry. Two series of saturated diacyl phosphatidylcholines, grouped according to their molecular weights of 678 and 706, with a total number of 25 molecular species were examined. The normalized acyl chain-length difference between the *sn*-1 and *sn*-2 acyl chains for a given phospholipid molecule in the gel-state bilayer is expressed quantitatively by the structural parameter $\Delta C/CL$, and the values of $\Delta C/CL$ for the two series of lipids under study vary considerably from 0.04 to 0.67. When the value of $\Delta C/CL$ is within the range of 0.09–0.40, it was shown that the thermodynamic parameters are, to a first approximation, a linear function of $\Delta C/CL$ with a negative slope. In addition, the experimental T_m values and the predicted T_m values put forward by Huang (Biochemistry (1991) 30, 26–30) are in very good agreement. Beyond the point of $\Delta C/CL = 0.41$, the influence of acyl chain-length asymmetry on the thermodynamic parameters deviates significantly from a linear function. In fact, within the range of $\Delta C/CL$ values of 0.42–0.67, the thermodynamic parameters in the T_m (or ΔH) vs. $\Delta C/CL$ plot were shown to be bell-shaped with the maximal T_m (or ΔH) at $\Delta C/CL = 0.57$. These results are discussed in terms of changes in the acyl chain packing modes of various phosphatidylcholine molecules within the gel-state bilayer in excess water.

Introduction

Phosphatidylcholines, quantitatively the most important lipids in animal cell membranes, are composed of a polar, zwitterionic headgroup and two hydrocarbon chains linked covalently to the glycerol backbone. It is the variety in the hydrocarbon chain length, the degree of unsaturation of the chain, and the presence of mono- or multi-branched chains that makes the family of phosphatidylcholines an extremely complex mixture of different molecular species.

The hydrocarbon chains in phosphatidylcholine molecules are derived biosynthetically from fatty acyl-CoA [1]. Most fatty acids hydrolyzed from naturally occurring phosphatidylcholines typically have even numbers of carbon atoms; however, phosphatidylcholines from some marine organisms contain odd numbers of carbons. In fact, variations in the length and structure of fatty acyl chains may amount to several hundred molecular species of phospholipids in membranes of most cells. At present, it is not known why membrane phospholipids have such a wide diversity of acyl chain lengths. However, it seems most likely that phospholipids with various chain lengths may confer a wide range of effective hydrocarbon thickness which, in turn, can match locally with the hydrophobic segments of different integral membrane proteins, resulting in stable, yet dynamical, lipid-protein complexes. Such dynamic associations may be the most expedient way for membrane lipids to modulate the functions and molecular dynamics of various integral membrane proteins in the two-dimensional plane of the lipid bilayer.

Abbreviations: C(X):C(Y)PC, saturated 1-α-phosphatidylcholine having X carbons in the *sn*-1 acyl chain and Y carbons in the *sn*-2 acyl chain; DSC, differential scanning calorimetry; M_r, molecular weight; T_m, main phase transition temperature; ΔH, transition enthalpy.

Correspondence: C. Huang, Department of Biochemistry, Box 440, Health Sciences Center, University of Virginia, Charlottesville, VA 22908, U.S.A.

Besides influencing the protein-lipid interactions, the heterogeneity of the acyl chain lengths also allows the assembly of phosphatidylcholines including the lipid bilayer to exhibit a wide range of physical properties in excess water. Of the many known physical parameters associated with the phospholipid bilayer, the main phase transition temperature, T_m, can be most accurately and reproducibly determined by high-resolution differential scanning calorimetry (DSC). This physical parameter is more important than just a mid-point temperature of the transition curve reflecting the melting of the lipid acyl chains in the bilayer; in addition, it also specifies a discrete temperature above which phosphatidylcholine molecules in excess water are fully hydrated and these hydrated molecules undergo spontaneous self-assembly to form enclosed multilamellar liposomes [2,3]. Hence, from an experimental point of view, it is necessary to know the T_m value, at least approximately, to prepare liposomes from phosphatidylcholines with various lengths of acyl chains.

The T_m values of slightly over 45 saturated diacyl phosphatidylcholines, determined by high resolution DSC, have been identified (Ref. 4 and the references cited therein). However, a total number of 324 saturated diacyl phosphatidylcholines exists, if each of the two acyl chains positioned at the *sn*-1 and *sn*-2 carbons of the glycerol backbone is limited to have a range of 9 to 26 carbon atoms. Clearly, our current knowledge about the T_m values of saturated diacyl phosphatidylcholines is far from complete. The present prospect of acquiring all the unknown values of T_m in the immediate future appears daunting, given the numerous and expensive organic syntheses and the painstaking and time-consuming DSC experiments that are required to perform. Hence, it seems that other avenue must be explored to yield the T_m values of saturated diacyl phosphatidylcholines.

Recently, Huang [4] made an attempt to predict empirically the T_m values of saturated diacyl phosphatidylcholines using the equation:

$$T_m = 154.2 + 2.0(\Delta C) - 142.8(\Delta C/CL) - 1512.5(1/CL)$$

where ΔC is the effective chain-length difference, in C-C bond lengths, between the two acyl chains for a phosphatidylcholine molecule in the gel state, CL is the effective length of the longer of the two acyl chains, also in C-C bond lengths, and $\Delta C/CL$ is the normalized chain-length difference between the *sn*-1 and *sn*-2 acyl chains. This equation was developed based on the existing data for fully hydrated phosphatidylcholines with $\Delta C/CL$ values in the range of 0.09–0.40 and it was suggested that this equation should be employed only to estimate the T_m values for those lipids with $\Delta C/CL$ values in the same range of 0.09–0.40. Despite this limitation, Huang was able to predict the T_m values of fully hydrated bilayers for 163 molecular species of saturated diacyl phosphatidylcholines.

In this communication, a relatively large number of saturated diacyl phosphatidylcholines have been semi-synthesized. One of our major aims of this work is to determine calorimetrically the T_m values of aqueous dispersions prepared from these synthesized phospholipids. By comparison with the predicted T_m values, we are able to address the question of how valid is the empirical equation of Huang as it applies to estimate the T_m values of saturated diacyl phosphatidylcholines. Furthermore, we can increase systematically the disparity between the two acyl chain-lengths in our synthesized lipids. The disparity or asymmetry of the lipid molecules is quantitatively expressed by the structural parameter $\Delta C/CL$. The second objective here is to gain further understanding into how the lipid bilayers comprised of various asymmetric phosphatidylcholines respond to the systematic change in $\Delta C/CL$ as they undergo the reversible main phase transitions. Finally, it has been well established that many asymmetric phosphatidylcholines can self-assemble into the mixed interdigitated bilayer, in excess water, at $T < T_m$ (Ref. 5 and the references cited therein). Our final aim here is to analyze the phase behavior exhibited by aqueous dispersion prepared from our synthesized saturated diacyl phosphatidylcholines and, based on the results, to define a range of $\Delta C/CL$ values within which the mixed interdigitated packing mode is most likely adopted by the asymmetric phosphatidylcholines in the bilayer at $T < T_m$. Consequently, the importance of the structural parameter ($\Delta C/CL$) in distinguishing the two types of gel-state bilayers, i.e., the partially interdigitated and mixed interdigitated bilayers, can be better understood.

Materials and Methods

Materials

Fatty acids and lysophosphatidylcholines with different chain lengths were purchased from Sigma (St. Louis, MO) and Avanti Polar Lipids, Inc. (Alabaster, AL), respectively. Saturated diacyl mixed-chain phosphatidylcholines were synthesized from fatty acids and lysophosphatidylcholines using catalyst 4-pyrrolidinopyridine and were purified by silica gel column chromatography as previously reported [6].

Sample preparation

Aqueous lipid dispersions for DSC experiments were prepared by incubating 3–5 mM lipid in 50 mM NaCl aqueous solution containing 5 mM phosphate buffer and 1 mM EDTA (pH 7.4) in a total volume of 2–3 ml. The sample was subject to heating/cooling cycles between 0°C and 10°C above the T_m, estimated from Ref. 4, three times. The sample was then cooled to 0°C and

stored at 0°C under N_2 atmosphere for a minimum of 5 days, if not specified otherwise, prior to DSC experiments. After 0°C incubation, the sample was first degassed and then placed into the sample cell of the calorimeter which had been preequilibrated thermally at the desired temperature (usually 4°C). Prior to the DSC initial heating run, the sample was further incubated in the calorimeter for 1 h at the desired temperature.

Differential scanning calorimetry (DSC)

All DSC measurements were made with a high-resolution MC-2 differential scanning microcalorimeter with cooling capability interfaced to an IBM microcomputer (Microcal Inc., Northampton, MA). The calorimetric data were collected and stored automatically by the microcomputer using the DA-2 digital acquisition system provided by Microcal. Each sample was scanned at least four times: two heating and two cooling runs at a nominal scan rate of either 10 or 15 C°/h. Prior to cooling and immediated reheating, the sample was thermally equilibrated in the calorimeter cell for 30 and 60 min, respectively.

Assignments of the main phase transition and its temperature (T_m)

It is now well known that the peak area and peak position of the main endothermic transition or the gel to liquid-crystalline phase transition exhibited by aqueous dispersions of lipids in the DSC repeated heating and cooling curves obtained at a constant slow scan rate of either 10 or 15 C°/h are virtually identical; moreover, the transition peak of the main phase transitions is also considerably sharper and larger than those of the sub- and pretransitions [6–8]. Based on the reversible feature of the relatively sharp and large transition observed in the repeated DSC heating and cooling scans, the main phase transitions for all lipid dispersions under study were assigned. In the case that the cooling capability of the DSC is not available, it is important to point out that a direct transition of lipid lamellae from the subgel or crystalline phase to the liquid-crystalline or fluid phase (the $L_c \rightarrow L_\alpha$ transition) is known to take place for some short chain phospholipids [6,8], and the calorimetric criteria just given for the main phase transition in the repeated DSC heating scans can be fulfilled by the $L_c \rightarrow L_\alpha$ transition. In this type of transition, however, the formation of L_c phase occurs mainly at the supercooling temperature, and the $L_c \rightarrow L_\alpha$ endothermic transition is accompanied by an unusually large transition enthalpy [6–8]. Such characteristic transition enthalpy can be drastically reduced, if the sample is rescanned calorimetrically from an initial preincubation temperature which is only a few degrees (5–10 C°) lower than the onset temperature of the suspected $L_c \rightarrow L_\alpha$ phase transition. Hence, the main phase transition can be distinguished from the $L_c \rightarrow L_\alpha$ phase transition by scanning the sample at different temperature intervals, even if the calorimeter can be used in the ascending temperature mode only. The transition temperature, T_m, of the assigned main phase transition was obtained from the endothermic peak in the DSC curve at the maximal excess heat capacity and the transition enthalpy (ΔH) was calculated from the area under the endothermic peak using the software subroutines provided by Microcal.

Results

The main phase transition behavior of saturated diacyl phosphatidylcholines with a common molecular weight of 678.0

Fig. 1 shows some representative thermograms for aqueous dispersions of 12 different molecular species of saturated diacyl phosphatidylcholines. The total number of chain methylene units in these 12 lipids is the same, i.e. 24, which is identical with that in C(14):C(14)PC. However, the molecular shapes of these lamellar lipids are quite different as the values of $\Delta C/CL$ vary considerably from 0.04 to 0.64. It should be reminded that an increase in $\Delta C/CL$ is an indication of increasing disparity or asymmetry between the two lipid acyl chains in the lipid molecule in the gel state bilayer [4,5].

C(13):C(15)PC ($\Delta C/CL = 0.040$)

The high-resolution DSC thermograms obtained with C(13):C(15)PC dispersions, as depicted in the bottommost curves in Figs. 1A, B, and C, show clearly the appearance of a sharp transition in all three DSC scans. Repeated DSC heating scans at various temperature intervals reveal that the sharp transition observed in the initial and successive DSC heating curves in the temperature range of 2 to 40°C, shown in Figs. 1A and C, is the $L_c \rightarrow L_\alpha$ phase transition with $T_m \approx 26.0$°C and $\Delta H = 12.8$ kcal/mol. The sharp exothermic transition at 25.5°C with a considerable smaller peak area ($\Delta H = 6.0$ kcal/mol) observed in the DSC cooling curve (Fig. 1B) is reversible upon reheating, provided that the sample has been thermally equilibrated in the calorimeter at a temperature above 10°C prior to reheating. Hence, this reversible transition at $T_m \approx 25.5$°C and $\Delta H = 6.0$ kcal/mol is assigned as the main phase transition (the $P_{\beta'} \rightarrow L_\alpha$ transition). A broad exothermic transition at 6.1°C with $\Delta H = 4.1$ kcal/mol is also discernible in Fig. 1B; this may be the $P_{\beta'} \rightarrow L_c$ phase transition.

C(14):C(14)PC ($\Delta C/CL = 0.115$)

The thermotropic phase behavior of C(14):C(14)PC after prolonged low-temperature incubation has been

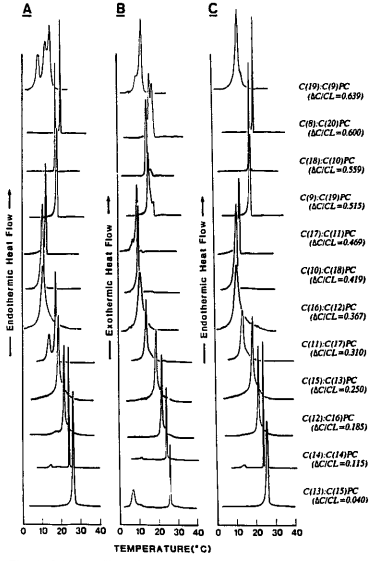

Fig. 1. DSC profiles of aqueous lipid dispersions prepared from various saturated diacyl phosphatidylcholines with a common M_r of 678. The values of $\Delta C/CL$ for these phospholipids are given, and the DSC thermograms are arranged in the order of increasing value of $\Delta C/CL$, i.e., in the order of increasing asymmetry of lipid acyl chains. (A) The initial heating scans. (B) The first cooling scans. (C) Immediate reheating scans. The scan rate was either 10 or 15 C°/h. Although all thermograms are placed on a common scale of temperature, the vertical scale is not the same for all thermograms.

well documented [8,9]. As shown in Fig. 1A, the aqueous dispersion of C(14):C(14)PC exhibits a main phase transition at 24.1°C (ΔH = 6.0 kcal/mol) and a small pretransition ($L_{\beta'} \rightarrow P_{\beta'}$) at 14.2°C ($\Delta H$ = 1.1 kcal/mol) upon initial DSC heating of the sample which has been preincubated at −20 °C for 6 h followed by 0°C-preincubation for 24 h. The main phase transition is reversible upon cooling and immediate reheating (Figs. 1B and C). However, the pretransition is first shifted downward in temperature by 3.3 C° upon cooling (Fig. 1B), and then shifted upward in temperature to 13.8°C upon immediate reheating (Fig. 1C), indicating that the transition temperature of the pretransition is prone to marked temperature hysteresis.

C(12):C(16)PC ($\Delta C/CL$ = 0.185)

The initial DSC heating thermogram of an aqueous dispersion of C(12):C(16)PC shown in Fig. 1A exhibits a symmetric endothermic transition at 21.7°C with ΔH = 5.7 kcal/mol and a very small endothermic transition at 17.0°C (ΔH = 1.25 kcal/mol). The larger transition at 21.7°C is the main phase transition, since it is reversible on subsequent cooling and reheating (Figs. 1B and C). The small transition is assigned as the $L_c \rightarrow P_{\beta'}$ transition, since it is abolished upon cooling and immediate reheating. It is perhaps pertinent to mention here that the lipid bilayer which undergoes the crystalline L_c phase to the rippled gel $P_{\beta'}$ phase transition without involving the intermediate step of $L_{\beta'}$ phase has been observed for a large number of mixed-chain phosphatidylcholines [10,11].

C(15):C(13)PC ($\Delta C/CL$ = 0.250)

Aqueous dispersions of C(15):C(13)PC show only a single endothermic transition in the temperature range of 2 to 35°C, even after prolonged incubation at 0°C for 34 days. This single transition at 18.8°C (ΔH = 5.3 kcal/mol) is also observed in the subsequent cooling and reheating thermograms (Fig. 1B and C). However, the transition enthalpy detected in the DSC cooling curve is reduced slightly by about 0.9 kcal/mol.

C(11):C(17)PC ($\Delta C/CL$ = 0.310)

The initial DSC heating thermogram for a sample of C(11):C(17)PC which has been preincubated at 0°C for 10 days is illustrated in Fig. 1A. In this figure, two partially overlapped endotherms peaked at 13.8 and 17.4°C with a total ΔH of 9.3 kcal/mol are observed. With longer preincubation periods, the high-temperature endothermic transition is observed to grow in both the peak height and peak area at the expenses of the low-temperature endothermic transition. Interestingly, the high-temperature transition at 17.4°C disappears upon cooling and immediate reheating (Figs. 1B and C), indicating that it is a subtransition as previously assigned [12]. In contrast, the low-temperature transition at 13.8°C reappears in the cooling and immediate reheating DSC curves (Figs. 1B and C). Moreover, the transition enthalpy of this low-temperature transition is virtually constant (ΔH = 4.9 kcal/mol) in all subsequent repeated heating and cooling scans. Consequently, this low-temperature transition is assigned as the main phase transition.

C(16):C(12)PC ($\Delta C/CL$ = 0.367)

On initial DSC heating, C(16):C(12)PC dispersions exhibit a single transition at 11.3°C with ΔH = 4.5 kcal/mol in the temperature range of 2 to 30°C (Fig. 1A). This transition temperature is reversible on cooling or immediate reheating; however, the value of ΔH

is decreased by about 0.9 kcal/mol in the cooling thermogram.

C(10):C(18)PC ($\Delta C/CL = 0.419$) and C(18):C(10)PC ($\Delta C/CL = 0.559$)

These two asymmetric phospholipids are known from X-ray diffraction studies to self-assemble in excess water into the mixed interdigitated gel bilayers at $T < T_m$ [13–16]. In addition, the thermotropic phase behavior of aqueous dispersions prepared from these two lipids has also been well characterized [15–19]. The calorimetric results of C(10):C(18)PC and C(18):C(10)PC shown in this work as illustrated in Fig. 1 are similar to those reported previously.

Basically, the aqueous dispersion of C(10):C(18)PC after prolonged preincubation at 0°C exhibits calorimetrically a single symmetric endothermic transition peaked at 11.1°C with $\Delta H = 6.2$ kcal/mol upon initial heating (Fig. 1A); this thermal transition has been previously assigned as the mixed interdigitated gel to the liquid-crystalline phase transition [16]. On immediate cooling, the same sample displays an asymmetric exothermic transition peaked at 10.1°C with $\Delta H = 5.6$ kcal/mol (Fig. 1B). The down-shift in T_m as well as a slight decrease in ΔH observed in the cooling scan probably reflects the slow kinetics of the phase transition from the liquid-crystalline state to the mixed interdigitated gel state. The endothermic transition exhibited in the second heating scan, however, is identical to that observed in the initial heating scan as shown in Figs. 1A and C.

Fully hydrated C(18):C(10)PC shows a sharp, single, symmetric, endothermic transition at 18.8°C with ΔH of 9.0 kcal/mol upon initial heating (Fig. 1A); this corresponds to the mixed interdigitated gel to the liquid-crystalline phase transition [15,17]. However, two partially overlapped exothermic transitions peaked at 17.6 and 14.9°C with a total ΔH of 8.7 kcal/mol are seen in the cooling scan (Fig. 1B). Immediate reheating shows a highly symmetric endothermic transition with T_m and ΔH values identical to those of the single endothermic transition observed in the initial DSC heating scan. The down-shift in T_m and the appearance of two exothermic transitions in the DSC cooling curve may be viewed as due to the slow kinetics of the liquid-crystalline → mixed interdigitated gel phase transition and the possible presence of an obligatory intermediate during the phase transition of lipid dispersions from the liquid-crystalline state to the mixed interdigitated state. However, we have just shown that the C(10):C(18)PC dispersion exhibits a single exothermic transition upon cooling, and this exothermic transition also corresponds to the reversal of the mixed interdigitated gel → liquid-crystalline phase transition. The proposed obligatory intermediate for the C(18):C(10)PC system may be present in only catalytic amounts for the C(10):C(18)PC system during the time course of the liquid-crystalline → mixed interdigitated gel phase transition; consequently, it cannot be detected calorimetrically. In any case, one can be certain that the phase transition that a C(18):C(10)PC bilayer takes upon heating from the mixed interdigitated gel state to the liquid-crystalline state involves a more direct and rapid pathway. Accordingly, this phase behavior is taken as an important characteristic in assigning the mixed interdigitated gel → liquid-crystalline phase transition for other lipids with large values of $\Delta C/CL$.

C(17):C(11)PC ($\Delta C/CL = 0.469$), C(9):C(19)PC ($\Delta C/CL = 0.515$), and C(8):C(20)PC ($\Delta C/CL = 0.600$)

As shown in Figs. 1A and C, aqueous dispersions of C(17):C(11)PC, C(9):C(19)PC and C(8):C(20)PC all display a sharp, single, endothermic transition on initial heating and immediate reheating; however, two partially overlapped exothermic transitions are observed on cooling (Fig. 1B). The thermotropic phase behavior of aqueous dispersions prepared from these three lipids is thus phenomenologically very similar to that of fully hydrated C(18):C(10)PC just described. In addition, the $\Delta C/CL$ values of C(17):C(11)PC, C(9):C(19)PC and C(8):C(20)PC are very close to the value of $\Delta C/CL$ for C(10):C(18)PC. Consequently, the observed single endothermic transitions for aqueous dispersions of C(17):C(11)PC, C(9):C(19)PC, and C(8):C(20)PC can be attributed to the same general pattern of endothermic transition observed for C(18):C(10)PC, corresponding to the mixed interdigitated gel → liquid-crystalline phase transition. It perhaps should be mentioned that mixed-chain phosphatidylcholines with $\Delta C/CL$ values in the range of 0.50 to 0.57 that are known to undergo the mixed interdigitated gel → liquid-crystalline phase transition are characterized calorimetrically by a single endothermic transition upon repeated heatings [19]. The T_m and ΔH values for aqueous dispersions of C(17):C(11)PC, C(9):C(19)PC and C(8):C(20)PC are 12.8°C, 19.6°C, 21.3°C and 6.9, 11.3, and 12.2 kcal/mol, respectively.

C(19):C(9)PC ($\Delta C/CL = 0.639$)

An aqueous dispersion of C(19):C(9)PC which has been preincubated at 0°C for 80 days displays multiple phase transitions in the temperature interval of 2–25°C upon initial DSC heating (Fig. 1A). On cooling and immediate reheating, asymmetric transition peaks with discernible shoulders are clearly seen (Figs. 1B and C). One transition peaked at 13.3 ± 0.1°C ($\Delta H = 8.5$ kcal/mol) is, however, observed in all three thermograms shown in Figs. 1A, B and C and in all subsequent repeated DSC heating and cooling curves. In addition, one small shoulder at 15.3°C is observed in the repeated heating curves and one at 10.5°C is seen

in the cooling curve. As mentioned earlier, the mixed interdigitated gel → liquid-crystalline phase transition is reversible upon repeated heating; however, it shifts appreciably upon cooling. The small peaks at 15.3°C and 10.5°C observed in the heating and cooling curves, respectively, may correspond to the mixed interdigitated gel → liquid-crystalline phase transition. The reversible peak at 13.3°C observed in all heating and cooling DSC curves is assigned as the $P_{\beta'} \rightarrow L_\alpha$ or the main phase transition based on the reversible feature observed in the heating as well as the cooling scans.

The main phase transition behavior of saturated diacylphosphatidylcholines with a common molecular weight of 706.0

Fig. 2 illustrates the initial heating, cooling, and immediate reheating thermograms for aqueous dispersions of 13 different phosphatidylcholines. These saturated diacyl phosphatidylcholines have a common M_r of 706.0, but their molecular shapes, as expressed by the structural parameter of $\Delta C/CL$, are quite different. The total number of methylene units in these lipids is the same, i.e. 26, which is two methylene units more than those shown in Fig. 1.

C(14):C(16)PC ($\Delta C/CL = 0.037$)

The initial DSC heating curve of a C(14):C(16)PC dispersion which has been preincubated at 0°C for 9 months displays two endothermic transitions in the temperature range of 20–45°C (Fig. 2A). The high-temperature transition peaked at 34.9°C ($\Delta H = 8.1$ kcal/mol) is reversible upon cooling and immediate reheating; hence, it can be readily assigned as the main phase transition or the $P_{\beta'} \rightarrow L_\alpha$ phase transition. The low-temperature transition at 30.1°C ($\Delta H = 7.7$ kcal/mol) is abolished completely on cooling and reheating (Figs. 2B and C). However, if the C(14):C(16)PC dispersion is allowed to incubate at 5°C for 1 h after cooling, the sample will display the low-temperature transition again with a smaller ΔH value in the DSC reheating curve. Hence, this low-temperature transition appears to involve the L_c phase. In fact, this low-temperature transition has been previously assigned based on X-ray diffraction data as the $L_c \rightarrow P_{\beta'}$ transition [10,11].

C(15):C(15)PC ($\Delta C/CL = 0.107$)

The initial DSC heating thermogram shows a sharp, symmetric, endothermic transition at 34.1°C ($\Delta H = 7.1$ kcal/mol) and three small partially overlapped endothermic transitions in the temperature interval of 17.0–26.0°C with a total ΔH of 4.3 kcal/mol. On cooling, two exothermic transitions at 20.9 and 34.0°C are observed (Fig. 2B). The high-temperature transition at 34.0°C is reversible on reheating; hence, it

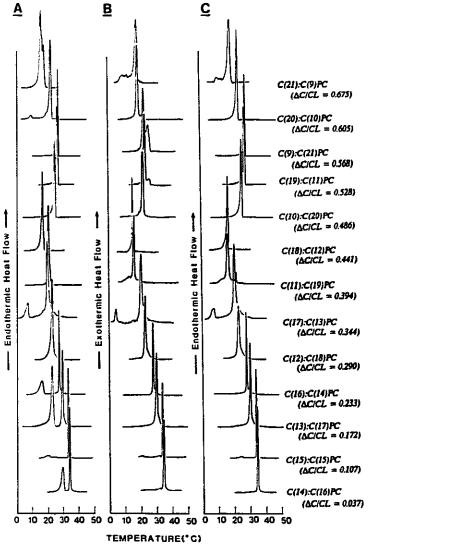

Fig. 2. DSC profiles of aqueous lipid dispersions prepared from various saturated diacyl phosphatidylcholines with a common M_r of 706. (A) The initial heating scans. (B) The first cooling scans. (C) Immediate reheating scans. See Fig. 1 legend for further explanation.

corresponds to the main phase transition. The low-temperature transition at 20.9°C is, however, shifted upward to 24.2°C upon reheating. This temperature hysteresis phenomena observed for the low-temperature transition is phenomenologically similar to the pretransition observed for C(14):C(14)PC; consequently, this low-temperature transition is assigned as the pretransition for the C(15):C(15)PC bilayer.

C(13):C(17)PC ($\Delta C/CL = 0.172$)

Two endothermic transitions of comparable transition enthalpies peaked at 23.6 and 30.5°C are observed in the initial DSC heating curve scanned from 5 to 50°C for C(13):C(17)PC. The high-temperature transition with ΔH of 6.9 kcal/mol is readily reversible on cooling and immediate reheating; consequently, it corresponds to the main or the $P_{\beta'} \rightarrow L_\alpha$ phase tranistion. The low-temperature endothermic transition at 23.6°C ($\Delta H = 7.6$ kcal/mol) disappears on cooling and reheating; it can be reasonably assigned as the $L_c \rightarrow P_{\beta'}$ phase transition.

C(16):C(14)PC ($\Delta C/CL = 0.233$)

The initial DSC heating thermogram for C(16):C(14)PC dipersions is characterized by two endothermic transitions peaked at 16.9°C ($\Delta H = 5.9$ kcal/mol) and 28.4°C ($\Delta H = 6.8$ kcal/mol). The broad low-temperature transition is irreversible upon cooling or immediate reheating. In contrast, the sharp high-temperature transition is independent of the thermal history, i.e., both the T_m and ΔH values of this high-temperature transition can be reproduced in the successive DSC cooling and reheating scans. It should be mentioned that the two endothermic transitions observed in the initial DSC heating scan have been reported previously; moreover, the low- and high-temperature transitions have been shown by X-ray diffraction studies to correspond to the $L_c \rightarrow P_{\beta'}$, and the $P_{\beta'} \rightarrow L_\alpha$ phase transition, respectively [10,11]. The T_m value of 28.4°C determined here is slightly larger than the average value of 27.2°C reported in the literature [20].

C(12):C(18)PC ($\Delta C/CL = 0.290$)

After 6 months of 0°C-preincubation, the C(12):C(18)PC dispersion exhibits a sharp and symmetrical endothermic transition peaked at 23.9°C with an unusually large enthalpy ($\Delta H = 13.0$ kcal/mol) in the temperature range of 13–38°C. On cooling or reheating, a single symmetric transition is again observed; however, the T_m is slightly down-shifted at 23.5°C and the value of ΔH is reduced appreciably ($\Delta H = 5.7 \pm 0.5$ kcal/mol). The large endothermic transition observed in the initial DSC heating scan and the smaller reversible transition observed after the first heating scan have been assigned previously as the $L_c \rightarrow L_\alpha$ and the $P_{\beta'} \rightarrow L_\alpha$ phase transitions, respectively [12].

C(17):C(13)PC ($\Delta C/CL = 0.344$)

The initial DSC heating curve of aqueous dispersions of C(17):C(13)PC scanned from 2 to 40°C exhibits two well resolved endothermic transitions peaked at 8.6 and 21.2°C with ΔH values of 1.2 and 5.2 kcal/mol, respectively (Fig. 2A). On cooling or reheating, the DSC thermogram for C(17):C(13)PC dispersions shows a high-temperature transition with T_m and ΔH values virtually identical to those of the corresponding high-temperature transition observed in the initial DSC heating scan; this demonstrates that the larger transition peaked at 21.2°C is the main phase transition. On cooling, the low-temperature transition at 8.6°C originally observed in the initial heating scan disappears; instead, a smaller transition at 5.1°C ($\Delta H = 0.4$ kcal/mol) is seen. It is quite possible that the low-temperature transition at 8.6°C is the $L_c \rightarrow P_{\beta'}$ phase transition, and that the formation of the more stable L_c phase could be sufficiently slow and incomplete during the time course of the DSC cooling scan.

C(11):C(19)PC ($\Delta C/CL = 0.394$)

Fig. 2A illustrates the initial DSC heating curve of an aqueous dispersion of C(11):C(19)PC which has been preincubated at 0°C for 5 months. This DSC curve from 5 to 45°C displays a single sharp endothermic transition peaked at 22.2°C with a small high-temperature shoulder at 22.7°C. The area under the endothermic peak is unusually large, corresponding to ΔH of 14.8 kcal/mol. On cooling, the large endothermic transition is replaced by a smaller asymmetric exothermic transition ($\Delta H = 4.4$ kcal/mol) with an apparent T_m at 17.3°C (Fig. 2B). On immediate reheating, two endothermic transitions peaked at 17.3 and 22.2°C are seen in the temperature interval of 5–45°C (Fig. 2C). If the sample is subject to further DSC heating scans starting from a higher temperature ($\geq$ 10°C), the low-temperature transition at 17.3°C ($\Delta H = 4.4$ kcal/mol) reappears, whereas the high-temperature transition at 22.2°C disappears in these repeated heating scans. Hence, the large endothermic transition at 22.2°C is most likely the $L_c \rightarrow L_\alpha$ transition, and the smaller reversible transition at 17.3°C is the main phase transition.

C(18):C(12)PC ($\Delta C/CL = 0.441$)

The molecular packings of C(18):C(12)PC in bilayers have been elucidated by X-ray diffraction technique [14,15]; in addition, the thermotropic phase behavior of aqueous dispersions of C(18):C(12)PC has also been well characterized [15,17,18]. A sample of C(18):C(12)PC which had been incubated at 0°C for 9.5 months was subject to DSC studies. The results are shown in Fig. 2. In the temperature interval of 5–32°C, an asymmetric endothermic transition peaked at 18.3°C with a low-temperature shoulder at 17.6°C is observed in the initial DSC heating curve. The overall ΔH for this overlapped peak is 13.7 kcal/mol. On cooling, two overlapped exothermic transitions peaked at 16.6 and 16.9°C with a total ΔH of 7.7 kcal/mol are discernible (Fig. 2B). On immediate reheating, a sharp, single endothermic transition at 17.5°C ($\Delta H = 8.4$ kcal/mol) is observed (Fig. 2C). This transition at 17.5°C is reproducible on subsequent repeated heatings; hence, it corresponds to the mixed interdigitated gel → liquid-crystalline phase transition. The high-temperature transition at 18.3°C observed only in the initial DSC heating curve corresponds to the $L_c \rightarrow L_\alpha$ phase transition [15,18]. The general transition pattern revealed in the cooling curve is very similar to that observed for C(18):C(10)PC, perhaps reflecting again the slow kinetics of the reversal of the mixed interdigitated gel → liquid-crystalline phase transition.

C(10):C(20)PC ($\Delta C/CL = 0.486$) and C(19):C(11)PC ($\Delta C/CL = 0.528$)

Similar to C(10):C(18)PC and C(18):C(10)PC, the thermotropic phase behavior of aqueous dispersions of C(10):C(20)PC and C(19):C(11)PC is also very simple (Fig. 2). On heating, C(10):C(20)PC and C(19):C(11)PC dispersions display single endothermic transitions at 26.8°C ($\Delta H = 9.2$ kcal/mol) and 28.7°C ($\Delta H = 10.1$ kcal/mol), respectively. On cooling, a single exothermic transition at 23.0°C ($\Delta H = 9.2$ kcal/mol) and two partially overlapped exothermic transitions at 24.6 and 27.3°C (total $\Delta H = 8.9$ kcal/mol) are reproducibly observed for C(10):C(20)PC and C(19):C(11)PC, respectively. The simple endothermic transitions observed in the repeated DSC heating scans can be inferred as the mixed interdigitated gel → liquid-crystalline phase transition [19].

C(9):C(21)PC ($\Delta C/CL = 0.568$)

The DSC heating thermograms for C(9):C(21)PC dispersions, shown in Figs. 2A and C, are characterized by a sharp, single, symmetric, endothermic transition with $T_m = 29.3$°C and $\Delta H = 11.0$ kcal/mol. On cooling, the DSC thermogram, shown in Fig. 2B, displays two partially overlapped exothermic transitions peaked at 23.9 and 26.6°C with an overall ΔH of about 11.0 kcal/mol. The general transition pattern exhibited by C(9):C(21)PC upon repeated heating or cooling is thus identical to that exhibited by fully hydrated C(18):C(10)PC shown in Fig. 1. In addition, the values of $\Delta C/CL$ for C(9):C(21)PC and C(18):C(10)PC are 0.568 and 0.559, respectively, indicating that these two lipid molecules have a nearly identical chain-length asymmetry and that the respective lipid molecules would thereby be capable of interacting among themselves to attain similar packing structures in the gel-state bilayer at $T < T_m$. It is well established that the single phase transition observed in the heating thermogram for C(18):C(10)PC corresponds to the mixed interdigitated → liquid-crystalline phase transition [15,17]. The single phase transition at 29.3°C exhibited by C(9):C(21)PC can, therefore, be assigned as the mixed interdigitated → liquid-crystalline phase transition.

C(20):C(10)PC ($\Delta C/CL = 0.605$)

The initial DSC heating thermogram for a C(20):C(10)PC dispersion in the temperature range of 5–50°C displays a small endothermic transition at 12.1°C ($\Delta H = 0.4$ kcal/mol) and a large endothermic transition at 24.8°C ($\Delta H = 10.7$ kcal/mol) with a small low-temperature shoulder at 22.1°C (Fig. 2A). On cooling, the small transition at 12.1°C disappears; instead, two partially overlapped exothermic transitions at 23.6°C ($\Delta H = 0.8$ kcal/mol) and 20.4°C ($\Delta H = 9.1$ kcal/mol) are observed. Subsequent reheatings show a single endothermic transition at 24.9°C ($\Delta H = 10.8$ kcal/mol). This single endothermic transition at 24.9°C is assigned to the mixed interdigitated gel → liquid-crystalline phase transition. This assignment is based on the fact that the repeated heating scans show only a single and reproducible transition and the repeated cooling scans show two partially overlapped exothermic transitions. In addition, the T_m of the high-temperature exothermic transition is less than the T_m of the endothermic transition. These observed calorimetric features are the transition characteristics exhibited by many asymmetric phosphatidylcholines such as C(18):C(10)PC and C(22):C(12)PC which are known to undergo the mixed interdigitated gel → liquid-crystalline phase transition [6,19].

C(21):C(9)PC ($\Delta C/CL = 0.675$)

The initial DSC heating, cooling, and immediate reheating thermograms for an aqueous dispersion of C(21):C(9)PC which has been preincubated at 0°C for 285 days are illustrated in Figs. 2A, B and C. These thermograms clearly demonstrate that C(21):C(9)PC dispersions exhibit multiple phase transitions. A complete assignment of all these transitions is not possible based on DSC data alone. Nevertheless, one can assign the phase transition at 20.1°C ($\Delta H = 8.1$ kcal/mol) seen in all three thermograms illustrated in Figs. 2A, B and C as the main phase transition or the $P_{\beta'} \rightarrow L_{\alpha}$ phase transition. This transition is in fact observed in all subsequent DSC heating and cooling curves and is independent of the thermal history of the lipid dispersion.

Discussion

In this communication, we reported the thermotropic phase behavior of aqueous dispersions prepared from two series of saturated diacyl phosphatidylcholines. One series consists of 12 members of phosphatidylcholines, and they all have a common M_r of 678.0 which is identical with that of C(14):C(14)PC. The second series consists of 13 molecular species, and each member has a M_r (706) identical with that of C(15):C(15)PC. However, the values of $\Delta C/CL$ are varied progressively and systematically for these two series of phosphatidylcholines. There is an important reason why these two series of saturated diacyl phosphatidylcholines are chosen. Some of the lipids such as C(14):C(14)PC, C(10):C(18)PC and C(18):C(10)PC in the first series and C(14):C(16)PC, C(16):C(14)PC and C(18):C(12)PC in the second series have been well characterized by previous investigations [8–20]. The available information about the bilayer structures and calorimetric properties of these well studied lipids allows one to compare and hence to assist in assigning, at least in part, the structures and the corresponding

TABLE I

Phase transition parameters of various phospholipid dispersions

Phospholipid	ΔC/CL	The main phase transition			The mixed interdigitated gel to L_α phase transition		
		T_m (°C)	ΔH (kcal/mol)	ΔS (cal mol per k)	T_m (°C)	ΔH (kcal/mol)	ΔS (cal mol per K)
C(13):C(15)PC	0.040	25.5	6.0	20.1			
C(14):C(14)PC	0.115	24.1	6.0	20.5			
C(12):C(16)PC	0.185	21.7	5.7	19.3			
C(15):C(13)PC	0.250	18.8	5.3	18.2			
C(11):C(17)PC	0.310	13.8	4.9	16.3			
C(16):C(12)PC	0.367	11.3	4.5	15.8			
C(10):C(18)PC	0.419				11.1	6.2	21.8
C(17):C(11)PC	0.469				12.8	6.9	24.1
C(9):C(19)PC	0.515				19.6	11.3	38.6
C(18):C(10)PC	0.559				18.7	9.0	30.8
C(8):C(20)PC	0.600				21.3	12.2	41.4
C(19):C(9)PC	0.639	13.3	8.3	29.0	15.3		
C(14):C(16)PC	0.037	34.9	8.1	26.3			
C(15):C(15)PC	0.107	34.0	7.1	23.1			
C(13):C(17)PC	0.172	30.5	6.9	22.7			
C(16):C(14)PC	0.233	28.4	6.8	22.6			
C(12):C(18)PC	0.290	23.5	5.7	19.2			
C(17):C(13)PC	0.344	21.2	5.2	17.7			
C(11):C(19)PC	0.394	17.3	4.4	15.2			
C(18):C(12)PC	0.441				17.5	8.4	28.9
C(10):C(20)PC	0.486				26.8	9.2	30.7
C(19):C(11)PC	0.528				28.7	10.1	33.5
C(9):C(21)PC	0.568				29.3	11.0	36.4
C(20):C(10)PC	0.605				24.9	10.8	36.2
C(21):C(9)PC	0.675	20.1	8.1	27.6			

calorimetric properties of the closely related molecular species in these two series of saturated diacyl phosphatidylcholines.

The DSC thermograms shown in Fig. 1 and Fig. 2 clearly demonstrate the variation and complexity of the transition patterns exhibited by the various saturated diacyl phosphatidylcholines in excess water. We will not attempt to discuss all these multiple peaks in this paper but will restrict our attention to the main phase transition and the mixed interdigitated gel to the liquid-crystalline phase transition observed for the two series of lipids. The transition temperature, T_m, and the transition enthalpy, ΔH, associated with these transitions are summarized in Table I. It should be noted that the main phase transitions are assigned for all lipids with $\Delta C/CL$ values in the range of 0.03–0.40.

TABLE II

Comparison between experimental and predicted T_m values for saturated diacyl phosphatidylcholines with $\Delta C/CL$ values in the range of 0.10 to 0.40

Phospholipid	Mol. wt.	ΔC/CL	Observed T_m (°C) [a]	Predicted T_m (°C) [b]	Difference between the observed and predicted T_m (C°)
C(14):C(14)PC	678	0.115	24.1	24.4	−0.3
C(12):C(16)PC	678	0.185	21.7	20.7	+1.0
C(15):C(13)PC	678	0.250	18.8	17.5	+1.3
C(11):C(17)PC	678	0.310	13.8	14.6	−0.8
C(16):C(12)PC	678	0.367	11.3	12.0	−0.7
C(15):C(15)PC	706	0.107	34.0	33.9	+0.1
C(13):C(17)PC	706	0.172	30.5	30.3	+0.2
C(16):C(14)PC	706	0.233	28.4	27.1	+1.3
C(12):C(18)PC	706	0.290	23.5	24.2	−0.7
C(17):C(13)PC	706	0.344	21.2	21.6	−0.4
C(11):C(19)PC	706	0.394	17.3	19.3	−2.0

[a] Data obtained from Figs. 1 and 2.

[b] Values obtained from Ref. 4.

In contrast, the mixed interdigitated gel to liquid-crystalline phase transitions are assigned for the asymmetric phosphatidylcholines with $\Delta C/CL$ values in the range of 0.42–0.64.

One of the objectives of this work, as pointed out in the Introduction, is to establish the general validity of Huang's relationship in predicting the T_m values for saturated diacyl phosphatidylcholines with $\Delta C/CL$ values in the range of 0.09–0.40. The present studies provided additional experimental T_m values which can be compared with the predicted T_m values presented by Huang [4]. Table II demonstrates that the observed and the predicted T_m values are in very good agreement. It should be noted that among the eleven phospholipids tested, only three molecular species show deviations greater than 1°C between the experimental and the predicted T_m values; moreover, the largest discrepancy between the experimental and the predicted T_m values is only 2C° as shown for C(11):C(19)PC in Table II. In fact, discrepancies greater than 2 C° are often found in experimental T_m values for a given mixed-chain phosphatidylcholine obtained from different laboratories [20]. Thus, the good agreement between the experimental and the predicted data shown in Table II indicates that the basic assumptions and approaches used for predicting the T_m values of saturated diacyl phosphatidylcholines as adopted by Huang are basically valid.

The T_m values of the main phase transitions and the mixed interdigitated gel to the liquid-crystalline phase transitions for aqueous dispersions of phosphatidylcholines with various $\Delta C/CL$ values, shown in Table I, are plotted in Fig. 3 against their corresponding $\Delta C/CL$ values. Below the $\Delta C/CL$ value of 0.41, the T_m value is observed to decrease with increasing values of $\Delta C/CL$ values. In fact, within the range of $\Delta C/CL$ values of 0.1–0.4, the experimental T_m values are, to a first approximation, a simple linear function of the normalized chain-length asymmetry for each of the two series of phospholipids. In the case of the C(15):C(15)PC series, for instance, the averaged decrease in T_m is about 5.8 C° when the value of $\Delta C/CL$ is increased by 0.1. After the singular point of $\Delta C/CL = 0.41$, the shift in T_m reverses its direction, i.e., the T_m value now increases with increasing values of $\Delta C/CL$. However, a point of maximal T_m is reached at the $\Delta C/CL$ value of 0.56; thereafter, the T_m value drops again until the $\Delta C/CL$ value is about 2/3. A profile with the shape similar to those shown in Fig. 3 can be obtained, if the ΔH or ΔS values presented in Table I are plotted against $\Delta C/CL$.

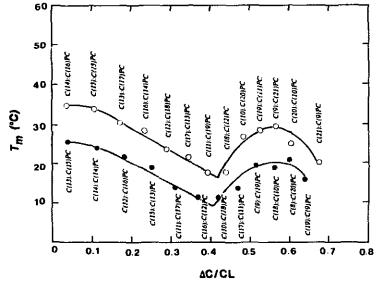

Fig. 3. Main phase transition temperature, T_m, as function of $\Delta C/CL$ for various saturated diacyl phosphatidylcholines with a common M_r of either 678 (solid circles) or 706 (open circles).

The values of transition temperature and transition enthalpy determined calorimetrically have been suggested to depend on the extent of intermolecular attractive interactions between lipid headgroups, the number of *gauche* conformations in the acyl chains, and the distance between the hydrocarbon chains in the gel-state lipid bilayer [21]. Since phosphatidylcholines with the same headgroup but different values of $\Delta C/CL$ are under current investigation, the observed change in the calorimetric parameters can be attributed to reflect primarily the variation in the conformational statistics of the hydrocarbon chain and the lateral chain–chain interactions in the gel-state bilayer. In the plot of T_m (or ΔH) vs. $\Delta C/CL$, the T_m (or ΔH) values are observed initially to decrease nearly linearly with increasing values of $\Delta C/CL$ (Fig. 3), implying that the conformational statistics of the hydrocarbon chain and the chain–chain lateral interactions of the lipid molecules in the gel-state bilayer are perturbed proportionally by a progressive increase in $\Delta C/CL$. This perturbation may be attributed to the bulky methyl ends of the lipid acyl chains [22]. As the value of $\Delta C/CL$ increases progressively, the two methyl ends within the same lipid molecule are gradually displaced further away from each other, resulting in progressively larger overlapping regions of the terminal methyl ends with the adjacent methylene groups of the lipid acyl chains in the closed packed gel-state bilayer. In these overlapping regions, the bulky methyl ends are expected to distort the all-*trans* conformation of the adjacent methylene units. Consequently, the packing order of the gel-state bilayer and the lateral chain–chain interactions are perturbed progressively by increasing the value of $\Delta C/CL$. When the value of $\Delta C/CL$ is increased to about 0.41, the magnitude of the perturbation becomes so overwhelming that the asymmetric phosphatidylcholine molecules in the bilayer at $T < T_m$ have to adopt a new equilibrium position, leading to a mixed interdigitated packing mode. In this new packing mode, the perturbing effects of the methyl ends of the longer acyl chains are effectively

removed. This is because the long acyl chains in the mixed interdigitated bilayer now span the whole width of the bilayer's hydrocarbon core; hence, the methyl ends at the long acyl chains are relocated near the interface between the hydrocarbon core of the bilayer and the two sides of aqueous media [5]. This relocating feature reverses the trend of the observed function in the plot of T_m (or ΔH) vs. $\Delta C/CL$, thereby resulting in a biphasic V-shaped segment of the experimental curve shown in Fig. 3.

The fact that beyond the singular point of $\Delta C/CL = 0.41$, C(9):C(21)PC ($\Delta C/CL = 0.57$) and a point between C(18):C(10)PC ($\Delta C/CL = 0.56$) and C(8):C(20)PC ($\Delta C/CL = 0.60$) show maximal T_m values, respectively, in the two bell-shaped curves shown in Fig. 3 may be interpreted as due to their stronger lateral chain–chain interactions in the mixed interdigitated bilayers. The mixed interdigitated bilayer is characterized by the long acyl chain extending completely across the bilayer span, whereas the two shorter chains, each from a lipid in the opposing leaflet, meet end-to-end in the bilayer midplane [5]. One can readily calculate that in the case of $\Delta C/CL = 0.57$–0.58, the sum of the effective chain lengths for the two opposing shorter acyl chains in their all-*trans*, zig-zag chain conformations plus the close van der Waals contact distance between two opposing terminal methyl groups (approx. 2Å) matches nearly perfectly with the effective overall chain length of the longer acyl chain in its all-*trans*, zig-zag chain conformation [19], thus permitting the maximal lateral chain–chain van der Waals contact interactions in the mixed interdigitated gel bilayer. On either side of the maximal value of T_m (or ΔH), asymmetric phospholipids with smaller or larger values of $\Delta C/CL$ such as C(18):C(12)PC cannot pack into the mixed interdigitated bilayers with their effective acyl chains in an all-*trans*, zig-zag conformations; kinks must be introduced into the aryl chains of these asymmetric phospholipids [14]. Consequently, the acyl chain packing order and the lateral chain-chain contact interactions are perturbed by the kinks, leading to smaller values of T_m (or ΔH).

The most asymmetric lipid in the two series of saturated diacyl phosphatidylcholines under study is C(21):C(9)PC ($\Delta C/CL = 0.675$). Our calorimetric data suggest that fully hydrated C(21):C(9)PC lamellae undergo the gel → liquid-crystalline phase transition, not the mixed interdigitated gel → liquid crystalline phase transition. It can be shown that the effective chain length of the longer C(21)-acyl chain of C(21):C(9)PC molecules in an all-*trans* conformation is 5.3 C-C bond lengths longer than the sum of the effective thickness of the two opposing shorter acyl chains, also in all-*trans* conformation, plus the van der Waals contact distance between two opposing methyl ends. In order to match laterally, in terms of the equivalent hydrophobic thickness, between the long acyl chain and the sum of two short acyl chains according to the packing mode of the mixed interdigitation, the long acyl chain cannot have an all-*trans* conformation; its length has to reduce by about 26.5%. This large decrease in the hydrophobic thickness corresponds approximately to the observed decrease in the bilayer hydrophobic thickness accompanied the gel to the liquid-crystalline phase transition for C(14):C(14)PC [23]. Hence, if the C(21):C(9)PC were self-assembled into the mixed interdigitated packing mode, the bilayer would have already transformed into the liquid-crystalline state with melted acyl chains. Clearly, the mixed interdigitated gel phase cannot be adopted by C(21):C(9)PC based on geometric considerations. As shown in Fig. 2, our repeated DSC scans of C(21):C(9)PC dispersions result in a reversible transition at 20.1°C, corresponding to the gel → liquid-crystalline phase transition. Accordingly, our DSC data can be inferred that the long acyl chain of C(21):C(9)PC molecule on one side of the bilayer packs end-to-end with the shorter chain of another C(21):C(9)PC molecule in the opposing bilayer leaflet at $T < T_m$.

In summary, aqueous dispersions of 25 saturated diacyl phosphatidylcholines have been studied by high-resolution DSC in the present work. These various phospholipds are grouped into two series according to their M_r of 678 and 706, respectively. Moreover, the various phospholipids with a common molecular weight within each of the two series can be arranged systematically according to their values of $\Delta C/CL$, a calculated structural parameter specifying the normalized chain-length difference between the two acyl chains of the phospholipid molecule in the gel state bilayer. To a first approximation, the T_m (or ΔH) value associated with the chain melting of the lipid bilayer appears to decrease linearly with increasing value of $\Delta C/CL$ up to $\Delta C/CL = 0.41$. Beyond $\Delta C/CL = 0.41$, the value of T_m (or ΔH) increases with increasing $\Delta C/CL$. However, within the range of $\Delta C/CL$ values of 0.42–0.67, the T_m (or ΔH) vs. $\Delta C/CL$ plot exhibits a bell-shaped profile with the maximal T_m (or ΔH) value at $\Delta C/CL \approx 0.57$. It is also inferred based on the phase transition behavior that the various asymmetric phosphatidylcholines in this range of $\Delta C/CL$ are self-assembled, in excess water, into the mixed interdigitated bilayers at $T < T_m$. At the point of $\Delta C/CL = 0.67$, the highly asymmetric phospolipids can no longer self-assemble into the mixed interdigitated gel bilayer due to the rather stringent geometry requirements for the lateral chain–chain interactions imposed by the packing mode of the mixed interdigitated gel bilayer. Although the T_m (or ΔH) values for saturated diacyl phosphatidylcholines with $\Delta C/CL$ values greater than 0.67 are not yet known, we advance the suggestion that the T_m (or ΔH) values will increase steeply with in-

creasing values of $\Delta C/CL$ for these highly asymmetric phospholipids. This suggestion is based on the high value of T_m known for the aqueous dispersions of C(18)-lysophosphatidylcholine (M_r = 523.7 and $\Delta C/CL = 1.15$). The aqueous dispersion of C(18)-lysophosphatidylcholine after prolonger incubation at 0°C has been well characterized to undergo the fully interdigitated bilayer → micellar transition at 26.0°C with ΔH = 7.0 kcal/mol [24].

Acknowledgements

This research was supported, in part, by a NIH grant, GM-17452, from U.S. Public Health Service, Department of Health and Human Services, and by an instrumentation grant, DiR-8907318, from the National Science Foundation.

References

1 Kennedy, E.P. (1986) in Lipids and Membranes: Past, Present and Future (Op den Kamp, J.A.F., Roelofsen, B. and Wirtz, K.W.A., eds.), pp. 171–206, Elsevier, New York.
2 Bangham, A.D., Standish, M.N. and Watkins, J.C. (1965) J. Mol. Biol. 13, 238–252.
3 Singer, M.A., Finegold, L., Rochon, P. and Racey, T.J. (1990) Chem. Phys. Lipids 54, 131–146.
4 Huang, C. (1991) Biochemistry 30, 26–30.
5 Huang, C. (1990) Klin. Wochenschr. 68, 149–165.
6 Lin, H.-n., Wang, Z.-q. and Huang, C. (1990) Biochemistry 29, 7063–7072.
7 Chen, S.C., Sturtevant, J.M. and Gaffney, B.J. (1980) Proc. Natl. Acad. Sci. USA 77, 5063–5063.
8 Lewis, R.N.A.H., Mak, N. and McElhaney, R.N. (1987) Biochemistry 26, 6118–6126.
9 Finegold, L. and Singer, M.A. (1986) Biochim. Biophys. Acta 855, 417–420.
10 Stümpel, J., Eibl, H. and Nicksch, A. (1983) Biochim. Biophys. Acta 727, 246–254.
11 Serrallach, E.N., De Haas, G.H. and Shipley, G.G. (1984) Biochemistry 23, 713–720.
12 Wang, Z.-q., Lin, H.-n. and Huang, C. (1990) Biochemistry 29, 7072–7076.
13 McIntosh, T.J., Simon, S.A., Ellington, J.C., Jr. and Porter, N.A. (1984) Biochemistry 23, 4038–4044.
14 Hui, S.W., Mason, J.T. and Huang, C. (1984) Biochemistry 23, 2775–2780.
15 Mattai, J., Sripada, P.K and Shipley, G.G. (1987) Biochemistry 26, 3287–3297.
16 Shah, J., Sripada, P.K. and Shipley, G.G. (1990) Biochemistry 29, 4254–4262.
17 Huang, C. and Mason, J.T. (1986) Biochim. Biophys. Acta 864, 423–470.
18 Boggs, J.M. and Mason, J.T. (1986) Biochim. Biophys. Acta 863, 231–242.
19 Xu, H. and Huang, C. (1987) Biochemistry 26, 1036–1043.
20 Keough, K.M.W. (1986) Biochem. Cell Biol. 64, 44–49.
21 Blume, A. (1979) Biochim. Biophys. Acta 557, 32–44.
22 Sisk, R.B., Wang, Z.-q., Lin, H.-n. and Huang, C. (1990) Biophys. J. 58, 777–783.
23 Janiak, M.J., Small, D.M. and Shipley, G.G. (1976) Biochemistry 15, 4575–4580.
24 Wu, W.-g., Huang, C., Conley, T.G., Martin, R.B. and Levin, I.W. (1982) Biochemistry 21, 5957–5961.